

## Supporting Information

# A Surface-Enhancement Raman Scattering Sensing Strategy for Discriminating Trace Mercuric Ion (II) from Real Water Samples in Sensitive, Specific, Recyclable and Reproducible Manners

*Bin Sun,<sup>‡</sup> Xiangxu Jiang,<sup>‡</sup> Houyu Wang,<sup>‡</sup> Bin Song, Ying Zhu, Hui Wang, Yuanyuan Su, and Yao He\**

Institute of Functional Nano & Soft Materials (FUNSOM) and Collaborative Innovation Center of Suzhou Nano Science and Technology, Soochow University, Suzhou, Jiangsu 215123, China.

Fax: (+86)-512-65880946

E-mail: [yaohe@suda.edu.cn](mailto:yaohe@suda.edu.cn)

**Enhancement factor (EF) calculation.** In detail, the EF value was calculated using the following well-established equation<sup>1-2</sup>:

$$EF = \frac{I_{SERS} \times N_{bulk}}{I_{bulk} \times N_{SERS}} \quad (\text{S-1})$$

Whereas,  $I_{SERS}$  and  $I_{bulk}$  are the intensity of the same Raman band for the SERS and bulk Raman spectra, respectively.  $N_{bulk}$  is the number of bulk molecules probed in a bulk sample, and  $N_{SERS}$  is the number of molecules adsorbed on the SERS active substrate. Thus, for SERS examination, a certain volume  $V_{SERS}$  of R6G aqueous solution was dispersed on an area of  $S_{SERS}$  at a concentration of  $C_{SERS}$  on the AuNPs@SiNWA<sub>r</sub> substrate. In contrast, a certain volume  $V_{bulk}$  of R6G aqueous solution was dispersed on an area of  $S_{bulk}$  at a concentration of  $C_{bulk}$  on the SiNWA<sub>r</sub> substrate. Both the substrates were dried in air. Foregoing equation thus comes:

$$EF = \frac{I_{SERS}}{I_{bulk}} \times \frac{S_{SERS} \times V_{bulk} \times C_{bulk}}{S_{bulk} \times V_{SERS} \times C_{SERS}} \quad (\text{S-2})$$

For objective calculation, Raman measurements were conducted under identical experimental conditions (laser wavelength, laser power, microscope objective/lenses, spectrometer, etc.).

**Calculation of limit of detection (LOD).** The LOD was estimated without  $\text{Hg}^{2+}$  ions giving SERS signal at least three times higher than background (DI water).<sup>3</sup> The standard curve of  $\text{Hg}^{2+}$  ions was plotted as

$$Y = A + B \times \text{Log}_{10} X \quad (\text{S-3})$$

where, A and B are the variable obtained via least-square root linear regression for the signal-concentration curve and variable  $Y$  represents the normalized SERS signal ( $I_{withHg^{2+}} / I_{BG}$ ) at  $Hg^{2+}$  concentration of  $X$  ( $C_{Hg^{2+}}$ ).

$$\text{When } Y = Y_{blank} + 3SD \quad (\text{S-4})$$

where,  $SD$  is the standard deviation and  $Y_{blank}$  is the SERS signal of blank sample (DI water).

$$\text{The } LOD \text{ was calculated as } LOD = 10^{[(Y_{blank} + 3SD)/Y_{blank} - A]/B} \quad (\text{S-5})$$

$SD$  was calculated according to the well-known formula:

$$SD = \sqrt{\frac{1}{n-1} \times \sum_{i=1}^n (X_i - X_{average})^2} \quad (\text{S-6})$$

where,  $n$  is the total number of the  $Hg^{2+}$  ions standard sample.  $X_i$  is the “ $i$ ” sample of the series of measurements.  $X_{average}$  is the average value of the SERS signals obtained for the specific series of identical samples repeated  $n$  times.

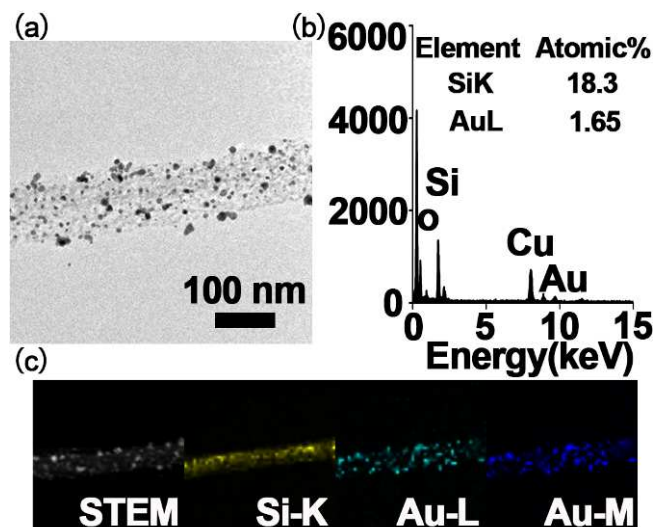


**Figure S1.** (a) TEM image of a single AuNPs@SiNW, (b) the elemental composition of the AuNPs@SiNW determined by energy-dispersive X-ray spectroscopy (EDS) and (c) its elemental mapping in the high-angle annular dark-field scanning TEM (HAADF-STEM). Inset in (b) represents the corresponding elemental ratio calculated by the EDS software. The TEM image shows a large amount of AuNPs with average sizes of 20 nm are uniformly decorated on the surface of the single SiNW. The EDX pattern indicates that the resultant AuNPs@SiNW contains Si and Au of 18.3 and 1.65% Atomic concentration, respectively, providing additional demonstration of the existence of Si and Au in the substrate. In addition, Si-K, Au-L, and Au-M are detectable in the HAADF-STEM image, further suggesting Si and Au elements are uniformly distributed in the AuNPs@SiNW.

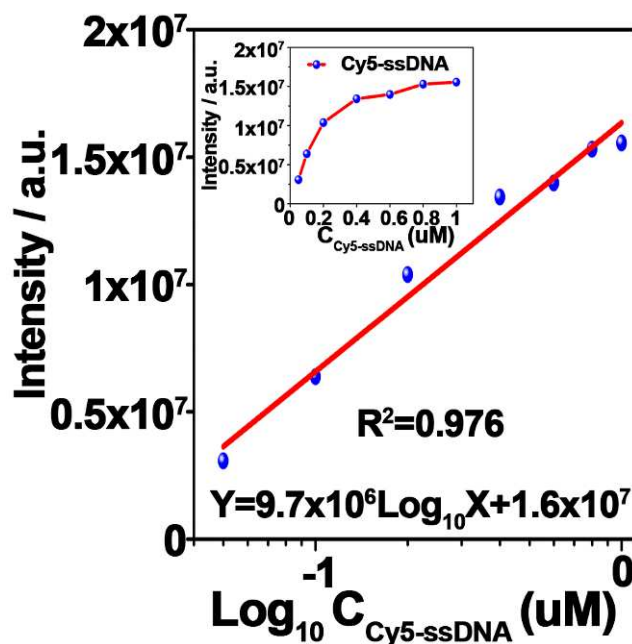


**Figure S2** .The linear fitting between the fluorescence intensity and logarithmic concentration of Cy5-ssDNA. The regression equation is  $Y = 9.7 \times 10^6 \text{Log}_{10} X + 1.6 \times 10^7$  with a correlation coefficient of 0.976, where Y represents fluorescence intensity and X represents  $C_{\text{Cy5-ssDNA}}$ , respectively. Inset presents the calibration curve of fluorescence intensity versus Cy5-ssDNA at different concentrations. According to the linear regression equation, it is readily calculated that  $\sim 17$  strands of Cy5-ssDNA are linked on the surface of one Au NP in AuNPs@SiNWAr

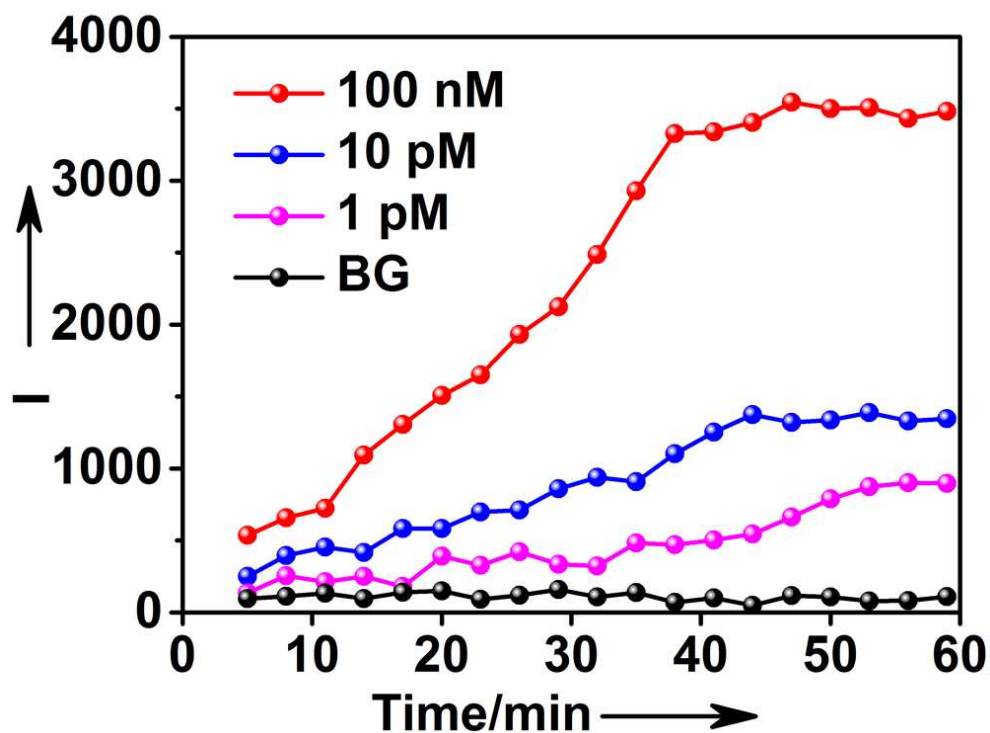


**Figure S3.** Kinetic studies of the developed SERS sensor at different  $\text{Hg}^{2+}$  concentrations of 0 (BG), 1 pM, 10 pM and 100 nM. Raman intensities of Cy5  $1366\text{ cm}^{-1}$  band are collected at the interval of 3 min. As shown in the Figure, the steady-state of reaction arrives at 35 min, 45 min and 55 min when  $\text{Hg}^{2+}$  concentration is 100 nM, 10 pM and 1 pM, respectively, indicating such kinetic property is also dependent on  $\text{Hg}^{2+}$  concentration, which is consistent with previous report.<sup>4</sup>

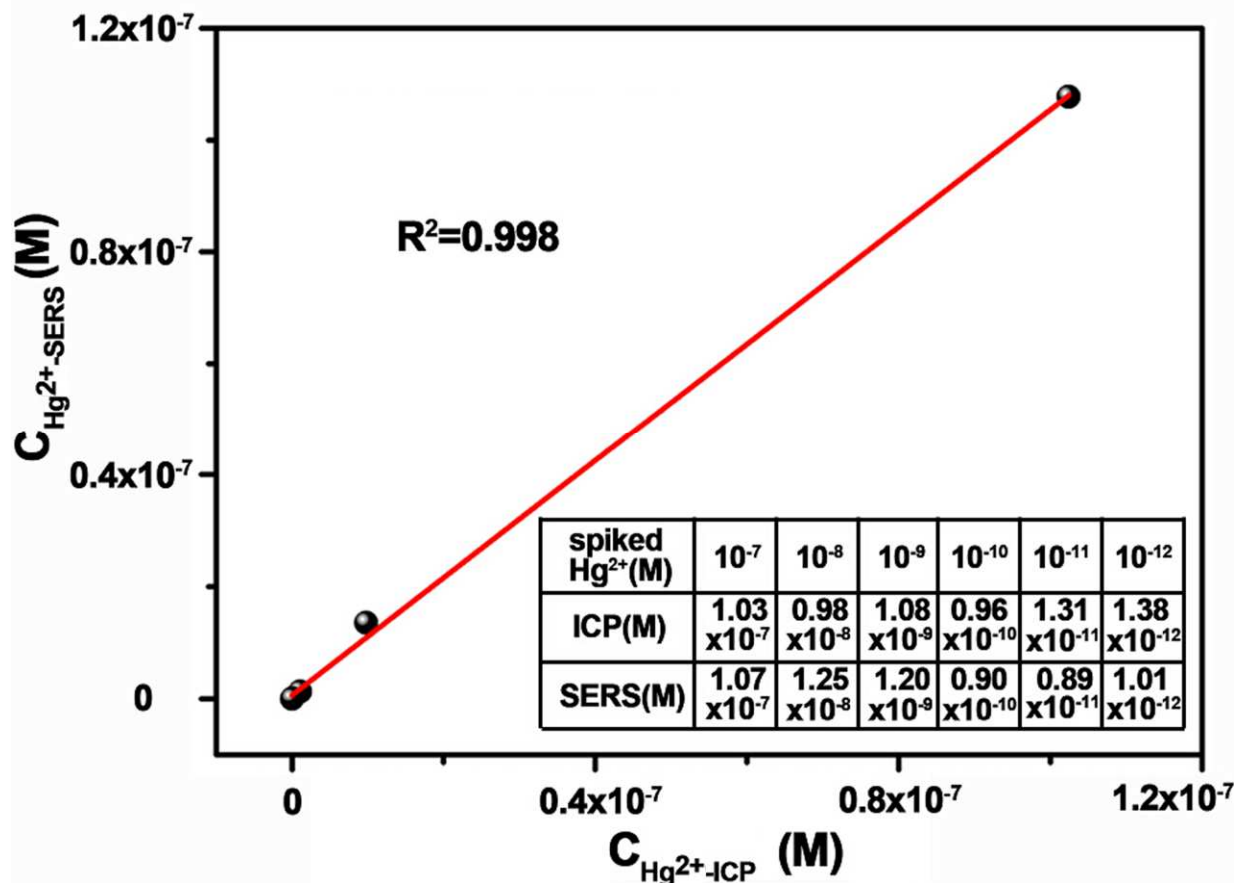


**Figure S4.** Hg<sup>2+</sup> concentrations in river water samples determined by the classic ICP-AES method and our SERS sensor. According to the linear fitting, there is a good correlation between the SERS sensor and ICP-AES, with the correlation coefficient  $R^2$  of 0.998, indicating the Hg<sup>2+</sup> concentrations detected by the SERS sensor are in good agreement with those determined by the ICP-AES strategy. For clear comparison, the values of Hg<sup>2+</sup> concentrations obtained from the standard addition analysis, determined by the ICP and SERS methods are listed in the inset table.

**Table S1.** Oligonucleotides sequences for DNA detection in the experiment.

| Oligonucleotides | Sequences                           |
|------------------|-------------------------------------|
| Stem-loop DNA    | 5'-Cy5-TTCTTTCTTCCCCTTGTTTGTT-SH-3' |
| Interfering DNA  | 5'-TGAGTGGACGTCAACGAGCAA-3'         |

---

**Table S2. Comparison of different SERS methods for the detection of Hg<sup>2+</sup>.**

| SERS substrate <sup>a</sup>   | Sensing mode | LOD <sup>b</sup> | RSD <sup>c</sup> | Ref.      |
|-------------------------------|--------------|------------------|------------------|-----------|
| AuNPs/grapheme heterojunction | Turn on      | 0.1 nM           | ~12%             | 5         |
| ZnO/Ag nano-arrays            | Turn off     | 2.25 nM          | ~17%             | 6         |
| Nanoporous Au film            | Turn off     | 1 pM             | not mentioned    | 7         |
| Au nanowire on Au film        | Turn on      | 100 pM           | not mentioned    | 8         |
| AuNPs@SiNWAr                  | Turn on      | 1 pM             | ~9%              | This work |

<sup>a</sup>AuNPs@SiNWAr, gold nanoparticles (AuNPs) decorated silicon nanowire array (SiNWAr). <sup>b</sup>LOD, limit of detection. <sup>c</sup>RSD, relative standard derivation, is served as the acknowledged indicator of reproducibility to evaluate whether it's good or not. Typically, RSD value less than 15% in the SERS method can be considered as good reproducibility.<sup>9,10</sup>

---

In summary, compared to previously reported results, our SERS sensor is quantifiably demonstrated to have both high sensitivity (LOD: 1 pM) and good reproducibility (RSD: 9%).

## REFERENCES

1. Jiang , X. X.; Jiang, Z. Y.; Xu , T. T.; Su, S.; Zhong, Y. L.; Peng , F.; Su , Y. Y.; He, Y. *Anal.Chem.* **2013**, *85*, 2809–2816.
2. Wang, H.; Jiang, X. X.; Wang, X.; Wei, X. P.; Zhu, Y.; Sun, B.; Su, Y. Y.; He, S. D.; He, Y. *Anal. Chem.* **2014**, *86*, 7368–7376.
3. Ma, W.; Kuang, H.; Xu, L. G.; Ding, L.; Xu, C. L.; Wang, L. B.; Kotov, N. A. *Nat Commun.* **2013**, *4*, 2689.
4. Li, D.; Wieckowska, A.; Willner, I. *Angew. Chem.* **2008**, *120*, 3991-3995.
5. Ding, X. F.; Kong, L. T.; Wang, J.; Fang, F.; Li, D. D.; Liu, J. H. *Appl. Mater. Interfaces* **2013**, *5*, 7072–7078.
6. Esmailzadeh Kandjani, A.; Sabri, Y. M.; Mohammadtaheri, M.; Bansal, V.; Bhargava, S. K. *Enviro. Sci. Technol.* **2014**, DOI: 10.1021/es503527e.
7. Zhang, L.; Chang, H. X.; Hirata, A.; Wu, H. K.; Xue, Q. K.; Chen, M. W. *ACS Nano* **2013**, *7*, 4595–4600.
8. Kang, T.; Yoo, S. M.; Yoon, I.; Lee, S.; Choo, J.; Lee, S. Y.; Kim, B. *Chem. Eur. J.* **2011**, *17*, 2211–2214.
9. Lee, C. H.; Hankus, M. E.; Tian, L.; Pellegrino, P. M.; Singamaneni, S. *Anal. Chem.* **2011**, *83*, 8953-8958.
10. Hankus, M. E.; Stratis-Cullum, D. N.; Pellegrino, P. M. ARL-TR-4957 September 2009.